Self-Arrangement of Molybdenum Particles into Cubes

A. S. EDELSTEIN, G. M. CHOW, E. I. ALTMAN, R. J. COLTON, D. M. HWANG

An unusual distribution of particle sizes has been observed following the formation of molybdenum particles by argon ion sputtering. Many of the molybdenum particles produced by sputtering at the threshold pressure for particle formation in the vapor appear to be single crystalline cubes. There are two prominent peaks in the edge length distribution of the cubes, one centered at 4.8 nanometers with a halfwidth of approximately 1.3 nanometers and the other at 17.5 nanometers. The peak for the larger cubes is approximately square and has a total width of 7.0 nanometers. Evidence is presented that the larger cubes are formed by a 3 by 3 by 3 self-arrangement of the smaller cubes, which contain approximately 7000 atoms. Self-arrangement in inorganic structures is normally only observed when the building blocks are atoms, molecules, or clusters of less than 100 atoms.

SELF-ARRANGEMENT IS COMMON IN nature and occurs in biology and when atoms crystallize. In nonorganic systems, individual atoms or molecules are usually the only building blocks. However, some NaCl clusters (*1*), containing as many as 100 atoms, form stable structures composed of six-atom rings. Here we report evidence that individual body-centered cubic (bcc), single crystalline Mo cubes with approximately 10 to 20 atoms on an edge, produced in the vapor by sputtering at high pressures, may self-arrange in the vapor into large cubes that are a 3 by 3 by 3 superstructure of the small cubes. The small Mo particles may act as the building blocks in forming the large cubes. Further, the small bcc Mo cubes, containing approximately 7000 atoms, are all aligned with their {100} faces parallel to one another in the large cubes.

We observed this unusual self-arrangement during a more extensive investigation (*2, 3*) of particle formation in the vapor. Particle formation in the vapor has been extensively studied (*4, 5*). For example, Chaudhari and Matthews (*5*) previously showed that their MgO crystallites have right-angle {100} faces and that there was zero twist angle between the crystallites in most clusters.

We sputtered Mo atoms at high Ar pressures so that the mean free path of the atoms is very short and they have many collisions with one another before reaching the substrate. If the density of atoms in the gas is high enough, that is, if the Ar pressure is above some threshold value, particles containing a thousand or more atoms will form in the vapor. If the Ar pressure is below this value, then the process is similar to conventional sputtering where atoms or small clusters of atoms are deposited on a substrate to form a film. We believe the reason for the existence of a threshold is related to the fact that particles are unstable unless the ratio of interior atoms to surface atoms is large enough (*6*). Thus, stable particles must be larger than some critical size, which is typically 2 to 5 nm. If there are not enough collisions, then the particles do not grow large enough to be stable.

We estimated (*3*) that the diffusion rate (velocity) of these particles in the Ar vapor to the substrate is only 10^{-2} cm s^{-1}. To increase the deposition rate, we set up a convective current in the Ar gas which then carries the particles to the substrate. This was done by cooling the substrate to liquid nitrogen temperatures, which creates a large temperature gradient between the substrate and the region near the target where the sputtering occurs (*7*). The substrate is an amorphous carbon film on a tungsten grid which was used in transmission electron microscope (TEM) measurements. The TEM measurements were performed using both a JEOL 200CX operated at 200 keV and a JEOL 4000FX high resolution TEM operated at 400 keV.

For Mo sputtered at 60 and 100 mtorr, the Mo is deposited as a film in which the individual grains grow in the form of columns perpendicular to the substrate (*8*). When the pressure is 150, 200, 300, 400, and 500 mtorr the deposition consisted solely of particles. Thus, there is a threshold pressure, approximately 150 mtorr, for particle formation to occur. For Mo sputtered at 200 mtorr or above, we observed most of the particles were nearly spherical in shape and they had the broad size distribution typical of particles grown in the vapor (*9*). For Mo sputtered at 150 mtorr, we found that both the particle shape and their size distribution are unusual. As illustrated in the TEM micrographs shown in Figs. 1 and 2, many particles have square projected areas. An examination of 202 particles in a TEM micrograph shows that there are two prominent peaks in the edge length distribution

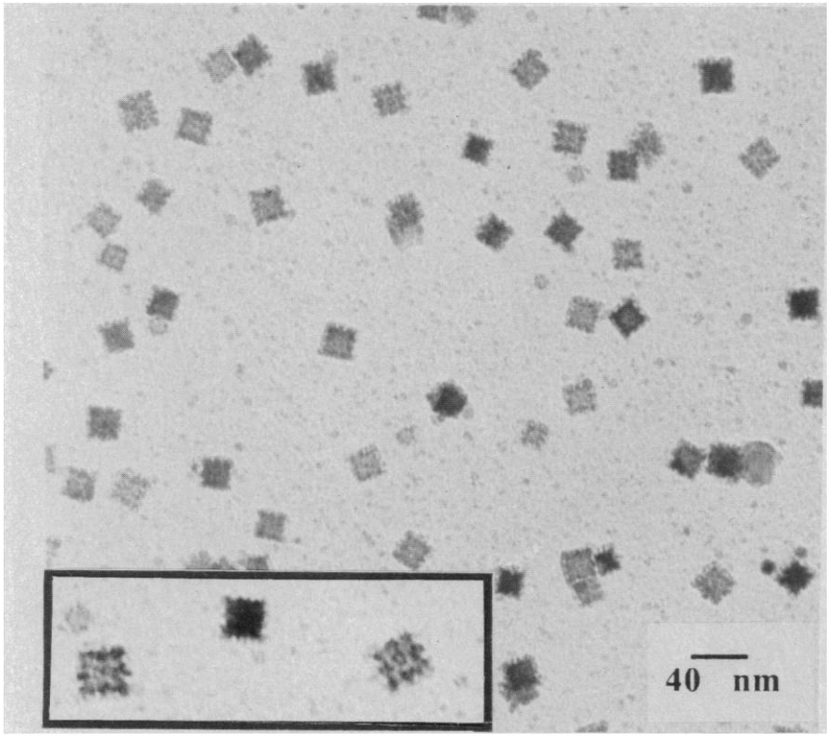

Fig. 1. TEM bright-field micrograph of the Mo particles sputtered in an Ar pressure of 150 mtorr which shows the 3 by 3 internal structure. The inset shows an enlarged view.

A. S. Edelstein, G. M. Chow, E. I. Altman, R. J. Colton, Naval Research Laboratory, Washington, DC 20375. D. M. Hwang, Bellcore, Red Bank, NJ 07701–7040.

of the cubes, one centered at 4.8 nm (corresponding to 15 unit cell lengths) with a halfwidth of approximately 1.3 nm, and the other at 17.5 nm. The peak for the larger cubes is approximately square and has a total width of 7.0 nm. Within this set, none of the particles had an edge length between 9 and 14 nm.

As shown in Fig. 1, the projected areas of the large particles are almost always squares. Based on symmetry considerations, we thought that the larger particles were cubes with their faces lying flat on the carbon substrate. We confirmed this by tilting the grid in an electron microscope and observing the expected hexagonal images of cubes viewed along a <111> direction. We also performed scanning tunneling microscopy, STM, measurements on films composed of these particles. The STM scans are consistent with the films containing some particles having flat faces and a vertical height of approximately 10 to 20 nm. Close examination of the projected images in Fig. 1 (see the inset of Fig. 1) shows that the large particles have a 3 by 3 internal structure.

Selected area electron diffraction patterns of the particles consist of polycrystalline diffraction rings and a diffuse background. The diffuse background is identical to that obtained from the amorphous carbon film of the TEM grid alone. The lattice spacings calculated from the diffraction rings agree to within 1% with the spacings of {110}, {200}, {112}, and {220} planes, of bulk bcc Mo. In high resolution micrographs, as shown in Fig. 3, we observed lattice fringes running diagonally across most of the large particles when the carbon film was in a horizontal orientation. The spacing determined from these fringes is 0.225 ± 0.002 nm which agrees with the {110} plane spacing of Mo. Since most large particles show crossed {110} fringes, for example (110) and (1$\bar{1}$0), the electron beam is along the [001] direction. From this we know that the large particles are lying flat or at most a few degrees away from lying flat with their {100} faces on the carbon film.

Due to their size and the reduced contrast, the small particles are not as well resolved as the large particles. There are at least as many small particles as large ones with square images as illustrated in Fig. 2. There are also many small particles with unresolved shapes. Many small particles also exhibited the 0.225-nm lattice fringes, but mostly only along one direction. We speculate that the small particles are mostly also cubes. However, due to the roughness of carbon substrate and the small cube faces, the small cubes may not always lie flat on the substrate with a principal axis pointing upward.

From the diffraction patterns and the lattice images we know that most of the particles are bcc Mo. Though amorphous phases would not have been detected because of the large background scattering off the amorphous carbon substrate, our measurements place an upper limit of 1% on the amount of a second crystalline phase.

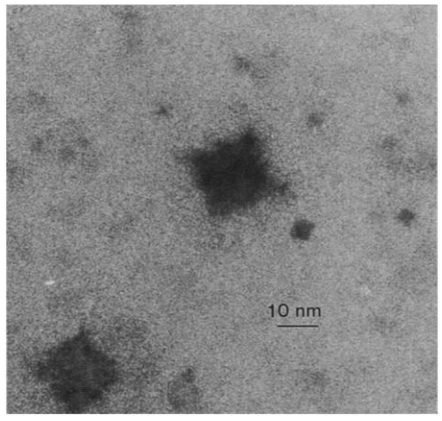

Fig. 2. TEM bright-field micrograph showing that the small particles appear to have square corners.

We have considered mechanisms for the growth of these particles in the vapor. At the threshold pressure, most of the Mo atoms may be utilized in forming particles of the critical size, that is, the smaller particles, and few are left over for further growth. In this case, further growth must proceed via collisions between the smaller particles. This is certainly possible since particle collision is a standard growth mechanism (*10*) for particles in the vapor phase. In this interpretation, the larger particles consist of a 3 by 3 by 3 arrangement of the smaller particles in a simple cubic superstructure. The internal structure seen in Fig. 1 arises from structural defects at the interfaces of the smaller particles which have not been completely annealed during coalescence. In some of the large particles, we can observe bending of the {110} lattice fringes which can be interpreted as nonperfect alignment between the smaller particles. The fact that the ratio of the average size of the large particles to that of the small particles is 3.6 is consistent with this superstructure model. There are possible reasons, such as nonperfect packing of the unequally sized, small particles, for the ratio being larger than 3. The alignment along {100} facets is similar to that observed by Chaudhari and Matthews for their MgO nanocrystals. In our case, because the colliding particles have a relatively narrow size distribution, it is possible that they can self-arrange after collision into a larger regular structure.

In the conventional growth mechanism the large particles would grow atom by atom. There are several things that are troublesome about this explanation. First, one would have expected to see a much more continuous size distribution for the particle sizes, rather than the bimodal distribution that we have observed. Secondly, the structure of the large cubes is very unusual.

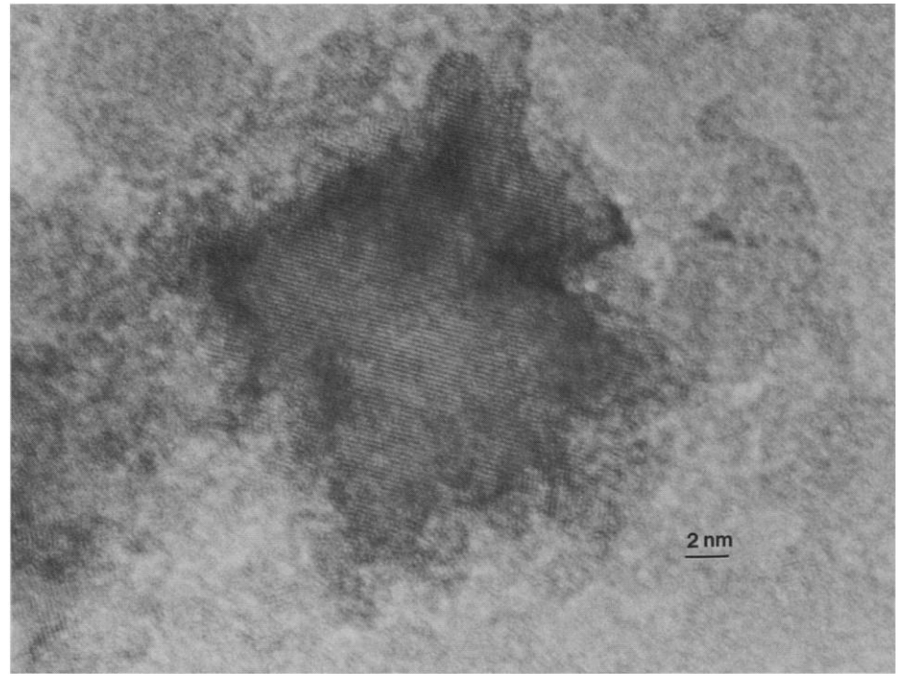

Fig. 3. High resolution TEM micrograph of one of the large Mo particles showing the {110} interference fringes.

Crystals usually grow (*11*) as regular polyhedra or as dendritic structures which may have dislocations but do not have the kind of regular 3 by 3 internal structure shown in Fig. 1.

There are obviously many unanswered questions. For example, why are the small metallic particles cubes? Why is the 3 by 3 by 3 superstructure of the large particles stable? In this connection it should be noted that in experiments (*12*) in which particles are formed by spraying atoms out of a nozzle, some configurations are much more stable than others.

REFERENCES AND NOTES

1. R. Pflaum, P. Pfau, K. Sattler, E. Recknagel, *Surf. Sci.* **156**, 165 (1985).
2. G. M. Chow *et al.*, *Appl. Phys. Lett.* **56**, 1853 (1990).
3. G. M. Chow, C. L. Chien, A. S. Edelstein, *J. Mater. Res.* **6**, 8 (1991).
4. For reviews see R. Uyeda, *J. Cryst. Growth* **24/25**, 69 (1974); C. Hayashi, *J. Vac. Sci. Technol. A* **5**, 1375 (1987).
5. P. Chaudhari and J. W. Matthews, *Appl. Phys. Lett.* **17**, 115 (1970).
6. F. F. Abraham, *Homogeneous Nucleation Theory* (Academic Press, New York, 1974).
7. A preliminary investigation indicates that the unusual particle formation is less prevalent if the substrate is not cooled.
8. Such columnar growth is typical when the substrate temperature is much less than the melting temperature.
9. R. A. Buhrman and C. G. Granqvist, *J. Appl. Phys.* **47**, 2200 (1976).
10. C. Kaito, *Jpn. J. Appl. Phys.* **17**, 601 (1978).
11. H. E. Buckley, *Crystal Growth* (Wiley, New York, 1961).
12. W. D. Knight *et al.*, *Phys. Rev. Lett.* **52**, 2141 (1984).

13. The authors gratefully acknowledge the Office of Naval Research for their financial support, J. M. Cowely for a portion of the electron microscopy study, R. K. Everett and E. McCormich for assistance, J. Karle and B. B. Rath for helpful discussions, and J. Karle, B. B. Rath, A. C. Ehrlich, S. C. Sanday, and D. J. Nagel for critical reading of the manuscript. This work was done while G.M.C. and E.I.A. were, respectively, research associates of the National Research Council and the Office of Naval Technology.

1 October 1990; accepted 6 February 1991

San Andreas Fault Zone Head Waves Near Parkfield, California

YEHUDA BEN-ZION* AND PETER MALIN†

Microearthquake seismograms from the borehole seismic network on the San Andreas fault near Parkfield, California, provide three lines of evidence that first *P* arrivals are "head" waves refracted along the cross-fault material contrast. First, the travel time difference between these arrivals and secondary phases identified as direct *P* waves scales linearly with the source-receiver distance. Second, these arrivals have the emergent wave character associated in theory and practice with refracted head waves instead of the sharp first breaks associated with direct *P* arrivals. Third, the first motion polarities of the emergent arrivals are reversed from those of the direct *P* waves as predicted by the theory of fault zone head waves for slip on the San Andreas fault. The presence of fault zone head waves in local seismic network data may help account for scatter in earthquake locations and source mechanisms. The fault zone head waves indicate that the velocity contrast across the San Andreas fault near Parkfield is approximately 4 percent. Further studies of these waves may provide a way of assessing changes in the physical state of the fault system.

EMERGENT FIRST ARRIVALS IN SEISmic records of earthquake monitoring networks often confuse efforts to interpret the initial ground motion caused by an earthquake. Emergent phases have been ascribed to various wave-propagation effects in the earth, such as refraction along horizontal layer boundaries and intrinsic attenuation of an otherwise sharp direct pulse. In this report, we discuss observational evidence for emergent first arrivals resulting from vertical material boundaries at a major crustal fault. On the basis of travel time and first motion polarity differences between emergent and sharp arrivals from Parkfield area earthquakes, we propose that the emergent arrivals are fault zone head waves refracted along the material contrast between the two sides of the San Andreas fault (*1–3*).

Figure 1 shows schematic ray paths of head waves and regular geometrical arrivals for subsurface receivers in a simplified fault zone geometry consisting of two quarter-spaces. In the higher velocity medium 1, there are two arrivals. The first is the direct wave, and the second is the wave reflected by the free surface. In the lower velocity medium 2, on the other hand, there are four distinct arrivals. The first is the head wave, the second is the direct wave, the third is a head wave reflected by the free surface, and the fourth is the free surface reflection of the direct wave.

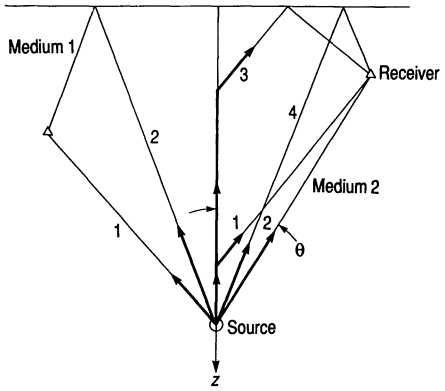

Fig. 1. Ray paths in faster (medium 1) and slower (medium 2) joined quarter-spaces; θ denotes the source-receiver angle used in Fig. 2.

The waveform character and motion polarity of head waves and direct arrivals are illustrated in Fig. 2. In the faster medium the first motion is that of a sharp direct wave, whereas in the slower medium gradual buildup of head wave amplitude produces an emergent pulse that precedes the sharp opposite polarity motion of the direct wave (*1*). In the absence of material contrast, the waves to the right of the fault are the reversed images of the sharp direct waves at corresponding points to the left of the fault.

To obtain field evidence for fault zone head waves, we examined seismograms from 75 microearthquakes in the Parkfield section of the San Andreas fault (*4*) (Fig. 3). The

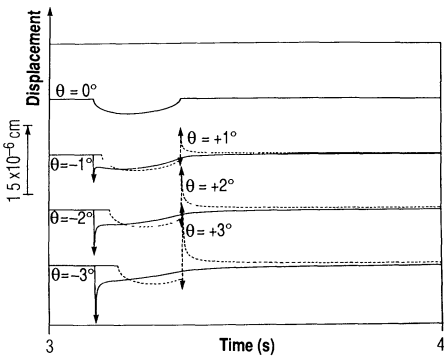

Fig. 2. Comparison of near-fault synthetic seismograms in faster (solid lines) and slower (dashed lines) joined quarter-spaces. Media velocities are 3.2 and 3.0 km/s, respectively. An antiplane line source dislocation of 1 cm operates at a depth of 10 km along the material interface at time = 0. Receivers are on the free surface at angular offset from the fault indicated by θ (positive clockwise). [Adapted from (*1*)]

Department of Geological Sciences, University of Southern California, Los Angeles, CA 90089 and Institute of Crustal Studies, University of California at Santa Barbara, CA 93106.

*Present address: Department of Earth and Planetary Sciences, Harvard University, 24 Oxford Street, Cambridge, MA 02138.
†Present address: Department of Geology, Duke University, Durham, NC 27706.